Water Mixing in a Tidal Current and the Effect of Turbulence on Tidal Exchange through a Strait

TOSHIYUKI AWAJI

Geophysical Institute, Kyoto University, Kyoto 606, Japan

(Manuscript received 9 December 1980, in final form 9 November 1981)

ABSTRACT

By means of numerical calculations of the Lagrangian movement of water particles released in a turbulent tidal current during three cycles of the M_2 tide, the mechanism of tidal mixing of the inner and outer waters divided initially by a strait and the effect of turbulence on tidal exchange through the strait are studied. In the vicinity of the strait, combined with the large Stokes drift due to the spatially rapid changes of the amplitude and the phase lag of the tidal current, turbulence strongly affects the Lagrangian movement of particles. Some of initially adjacent particles moving in a turbulent tidal current have much larger drifts than the Stokes drifts (non-turbulent) and the others much smaller drifts than those. As a result, the adjacent particles released in a turbulent tidal current are widely scattered, and they are well mixed with water particles initially far apart from them, i.e., local mixing of water amplified to a great extent occurs compared with that due only to turbulence. By the interaction of a large degree of local mixing induced by the Stokes drift and turbulence in the vicinity of the strait and the dynamic process of tidal exchange through the strait, the inner and outer waters are also well mixed with each other over an extensive area around the strait. With regard to the effect of turbulence on tidal exchange between two basins connected by the strait, turbulence has a minor influence on water volume exchanged through the strait, but it has a major influence on the enlargement of sea areas affected by tidal exchange. It is also shown that the dispersion coefficient evaluated from the variance of particle spread reaches 8×10^6 cm^2 s^{-1} in the vicinity of the strait.

1. Introduction

In order to arrive at estimates of tidally induced net exchanges of water between basins connected by a narrow strait, it has been necessary for many previous studies to invoke assumptions concerning the horizontal spread of intruding water and the physical process of mixing of the water with basin water, because the mechanism of tidal exchange through the strait was not clearly understood (Parker 1972; Kawamura *et al.*, 1975; and others).

Recently, Awaji *et al.* (1980) made a numerical experiment of tidal exchange through an idealized strait. They calculated the Lagrangian movement of a large number of labeled particles released in a tidal current during a full cycle of the M_2 tide according to the method known as the Euler-Lagrange problem (Longuet-Higgins, 1969), and evaluated the exchange ratio from the calculated distributions of the inner and outer waters initially divided by the strait. They clearly showed that tidal exchange through a strait is primarily induced by the spatially rapid changes of the amplitude and the phase lag of the M_2 current in the vicinity of the strait and it is developed by the combined action of the M_2 current and the tidally-induced residual current near the strait. In other words, large Stokes drifts of water particles in the vicinity of the strait cause the exchange of a large amount of water through the strait. In the study of Awaji *et al.* (1980) and also in the present study, the Stokes drift is defined as the Lagrangian drift over a cycle due to the spatial variability of all components of the Eulerian velocity field, i.e., the M_2 and tidally-induced residual currents. The reason is that the drift of a water particle cannot be divided into pieces induced by each component of the currents, because each component of the currents changes rapidly in space and in such a case the Euler-Lagrange transformation is strongly nonlinear (Zimmerman, 1976). The new method introduced by them has the advantage of allowing the evaluation of the exchange ratio without invoking any of the assumptions mentioned above, and also of easily investigating the mechanism governing water exchange through the strait.

For the purpose of simply revealing the physical mechanism of tidal exchange through a strait, Awaji *et al.* (1980) did not consider the turbulent motions of water particles. In actual seas there exists turbulence on various scales, and random motions of water particles due to turbulence are necessary for water mixing (Dyer, 1973). Then, if turbulent motions of water particles are taken into account, their new method is also very useful for the study of the

0022-3670/82/060501-14$07.50

physical process of water mixing in a tidal current, because water mixing is a Lagrangian phenomenon and should be investigated in a Lagrangian manner. Many studies have been made concerning tidal mixing, notably the studies based on shear dispersion (Bowden, 1965; Okubo, 1967; and others). In almost all of them, however, tidal mixing was investigated in an Eulerian manner, and the effect of the Stokes drifts of water particles on tidal mixing was not considered. As was clearly demonstrated by Awaji *et al.* (1980), large Stokes drifts (non-turbulent) are produced in the vicinity of the strait. Therefore it seems that in a turbulent tidal current, a large degree of water mixing is induced by the interaction of the large Stokes drifts and turbulence.

In the present study, water particles released in a turbulent tidal current are numerically tracked (in a turbulent tidal current random motions of particles due to turbulence are taken into account), and then, based on the relation between the calculated drifts in a turbulent tidal current and those in a non-turbulent tidal current (Stokes drifts), the physical manner of the Lagrangian movement of particles is investigated in order to understand the mechanism of local mixing of water in a Lagrangian manner. Next, the physical process of tidal mixing of the inner and outer waters and the effect of turbulence on tidal exchange through a strait will be studied.

2. Models

The model basin is the same as that used by Awaji *et al.* (1980, their Fig. 1). It consists of an inner and an outer basin connected to each other by a narrow strait 5 km in length and 4 km in width. The bottom of the basin is flat and is 40 m below mean sea level. The equations of motion and continuity of barotropic tide are

$$\frac{\partial \mathbf{u}}{\partial t} + \mathbf{u}\cdot\nabla_H\mathbf{u} + f\mathbf{k}\times\mathbf{u} = -g\nabla_H\zeta + \nu_H\nabla_H{}^2\mathbf{u} + \frac{\tau}{\rho_0(H+\zeta)}, \quad (1)$$

$$\frac{\partial \zeta}{\partial t} = -\nabla_H[(H+\zeta)\mathbf{u}], \quad (2)$$

where $\mathbf{u}$ denotes the horizontal Eulerian velocity vector with components u and v related to the horizontal coordinates x and y, respectively, ζ the surface elevation above mean sea level, H ($\approx$40 m) the depth of the bottom, f ($=0.77\times10^{-4}$ s^{-1}) the Coriolis parameter, g ($=980$ cm s^{-2}) the gravitational acceleration, ν_H ($=5.5\times10^5$ cm^2 s^{-1}) the constant eddy viscosity, τ [$=-0.0026\times|\mathbf{u}|\mathbf{u}$ (g cm^{-1} s^{-2})] the bottom stress, ∇_H the horizontal gradient operator, $\nabla_H{}^2$ the horizontal Laplacian operator, and $\mathbf{k}$ the vertical unit vector acting upward. The water motion is driven by the M_2 tide at the open boundary which is given by

$$\zeta = \zeta_b \sin\{(2\pi/T)t\}, \quad (3)$$

where ζ_b ($=90$ cm) and T denote the amplitude and the cycle of the M_2 tide, respectively.

Since the Lagrangian movement of water is surveyed by means of tracking labeled particles released in the tidal current, it is necessary to know their Lagrangian velocities. The Lagrangian velocity of a labeled particle in the present model consists of the velocity due to the tidal current, and that due to turbulence. The former is given by interpolating the Eulerian velocities of the tidal current calculated at every grid spacing of 1 km. The latter is given by random numbers numerically generated in every time-step according to a Markov-chain model described in the next section.

a. Numerical generation of turbulence

When considering numerical simulation methods of turbulent velocities experienced by particles, several kinds of random-walk models are well-known (Sullivan, 1971; Hall, 1975; and others). The Markov-chain model is the most convenient approach in the present model, because the calculation of particle motions must be performed at a small time interval (within a few minutes) so as to satisfy the Markov assumption; this model has the advantage that a sequence of turbulent velocities can be obtained very easily. The Markov-chain model was theoretically derived by Hall (1975). He clearly showed that the model was reasonable as a simulation model of turbulent velocities in the atmosphere. Applying this model to some coastal seas, Wada and Kadoyu (1976) also showed that the statistics of turbulence (e.g., an auto-correlation function and power spectrum) calculated from this model agreed closely with those observed in the coastal seas.

In the present study, two fields of turbulence (two-dimensional) are generated by this model in order to understand readily the fundamental roles of turbulence in water mixing and water exchange through the strait. One has the amplitude of the fluctuations corresponding to a turbulent diffusivity of 10^4 cm^2 s^{-1}, and the other has that corresponding to a turbulent diffusivity of 10^5 cm^2 s^{-1}. The integral time scale is taken to be 1.0 lunar hour. The above situations are determined according to the study of Wada and Kadoyu (1975) in which it was shown that representative turbulent diffusivities in the central parts of actual bays and in the vicinity of straits were $10^4 \sim 10^5$ cm^2 s^{-1} and $10^5 \sim 10^6$ cm^2 s^{-1}, respectively, and that the integral time scale of turbulence fields in bays was $\sim$1.0 lunar hour. The Markov-chain model is briefly described in the Appendix (the relation between the amplitude of tur-

bulent fluctuations and turbulent diffusivity is also shown).

b. The method of tracking labeled particles

Water particles are labeled so that they can be distinguished from one another. Imagine the nth labeled particle at the position $\mathbf{X}_n(t_i)$ at time t_i. Then, the new position $\mathbf{X}_n(t_{i+1})$ after a small time interval $\Delta t (t_{i+1} = t_i + \Delta t)$ is given by

$$\mathbf{X}_n(t_{i+1}) = \mathbf{X}_n(t_i) + \mathbf{u}'_n(t_i)\Delta t + \int_{t_i}^{t_{i+1}} [\mathbf{u}\{\mathbf{X}_n(t_i), t\} + \int_{t_i}^{t} \mathbf{u}\{\mathbf{X}_n(t_i), t'\}dt' \nabla_H \mathbf{u}\{\mathbf{X}_n(t_i), t\}]dt, \quad (4)$$

where $\mathbf{u}$ denotes the velocity vector at the position $\mathbf{X}_n(t_i)$ obtained from interpolating the Eulerian velocities of the tidal current calculated at every grid point (see Awaji *et al.*, 1980), and $\mathbf{u}'_n(t_i)$ denotes the turbulent velocity vector experienced by the nth labeled particle during the time t_i to t_{i+1}. The calculation of particle motions is started at the time of a maximum inward current at the center of the strait according to Imasato *et al.* (1980) so that the particles released initially in the strait can travel in both basins (the inner and outer basins) during a full cycle of the M_2 tide. Sixteen labeled particles are initially arranged in each grid box (Fig. 1), and then, using Eq. (4), they are tracked at a small time interval Δt ($\leqslant$3 min) so that the Markov assumption can be satisfied (Wada and Kadoyu, 1976). The calculations of particle motions is continued during three cycles of the M_2 tide.

3. Water mixing in the tidal current

With the object of understanding the roles of turbulence in water mixing and in tidal exchange through the strait, particle motions in the following three cases are calculated:

I. Particle motions driven only by the tidal current (no turbulence).

II. Particle motions driven by the tidal current and by turbulence numerically generated so as to give the equivalent diffusion coefficient of 10^4 cm^2 s^{-1}.

III. Particle motions driven by the tidal current and by turbulence numerically generated so as to give the equivalent diffusion coefficient of 10^5 cm^2 s^{-1}.

The calculated M_2 and tidally induced residual currents are the same as those of Awaji *et al.* (1980). The features of the M_2 current are as follows. Both the amplitude and the phase lag are rapidly changed in the vicinity of the strait. The velocity of the M_2 current exceeds 2.5 m s^{-1} in the strait. The phase lag

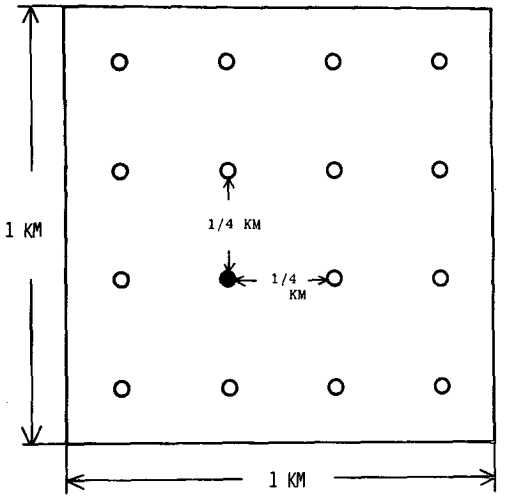

FIG. 1. The initial arrangement of labeled particles (16 particles) in a grid box. The particle denoted by a black circle is selected as the specified particle described in Section 3b.

of the v component takes over 6 lunar hours between both ends of the strait. In the velocity field of the tidally induced residual current, remarkable vortices exist in the neighborhood of the strait, and the maximum speed is 0.6 m s^{-1}.

Fig. 2 shows the time changes of the calculated distributions of labeled particles in the above three cases during three cycles of the M_2 tide, where small black squares represent the inner water particles released initially in the inner basin, and small open circles the outer water particles released initially in the outer basin. In the first tidal cycle the calculated distributions of labeled particles are shown at intervals of 3 lunar hours, and in the second and the third tidal cycles they are shown at 3 and 12 lunar hours of each tidal cycle. It is clearly seen in Fig. 2 that in every case large amounts of water are exchanged through the strait during a cycle. Fig. 2a (case I; the non-turbulent case) indicates that the particles in the vicinity of the strait are moving in a fairly complex way, and their distributions are observed as if the inner and outer waters were mixed together, although the phenomenon of water mixing should never occur in nonturbulent cases. The particles in areas far from the strait are moving regularly because the tidal current has only a small spatial change in those areas. Figs. 2b and 2c (cases II and III, respectively) show, however, that particles in the turbulent cases are irregularly scattered even in areas far from the strait.

a. Local mixing of water

Prior to the discussion about an important problem of the mixing of the inner and outer waters, local mixing of water in the tidal current is investigated, because it will facilitate understanding of the phys-

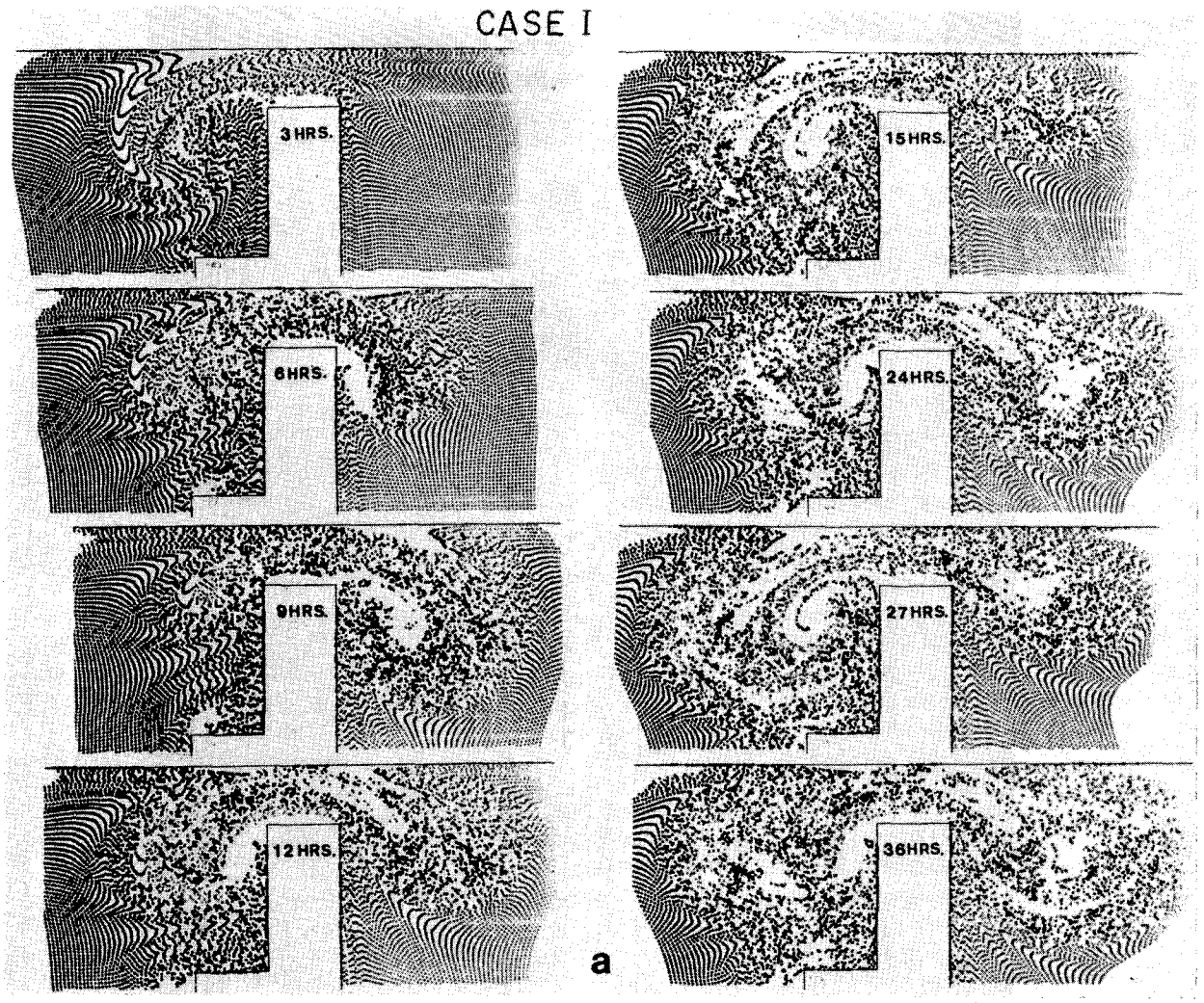

FIG. 2. The time-changes of the calculated distributions of labeled particles: (a) case I, (b) case II and (c) case III. The black squares represent the inner water particles released initially in the inner basin, and the open circles represent the outer water particles released initially in the outer basin.

ical process of the mixing of the inner and outer waters.

Local mixing of water defined in the present study is as follows. Water mixing is a Lagrangian phenomenon; hence local mixing of water should be studied in a Lagrangian manner. The water mixing in a square of fairly small area which is moved together with a specified particle is considered in this study. The particle shown in each grid box by a black circle in Fig. 1 is chosen as the specified particle, and it is always located in the center of the square (it must be noted that a square does not mean a grid box used in the calculation of the Eulerian tidal velocity). As both a square and water particles move in the tidal current, some of the particles initially in a square remain in the square and others go out from it, after time t, and water particles initially outside the square intrude into the square. In this situation, local mixing of water is defined as the mixing of the remaining water particles and the intruding ones in the square.

The mixing ratio M_R representing the degree of local mixing at time t is defined as

$$M_R = N_I(t)/N_A(t), \tag{5}$$

where $N_I(t)$ denotes the number of particles initially outside the square ($t = 0$) but inside the square at time t, and $N_A(t)$ the total number of particles included in the square at time t. The specified particle is excluded from N_I and N_A so that the value of M_R changes from 0 to 1. It should be noticed that the square is not fixed in space but moves with the specified particle for the purpose of evaluating the degree of local mixing in Lagrangian manners. In order to obtain a reasonable estimate of M_R, more than 50 particles should be included in every square; thus

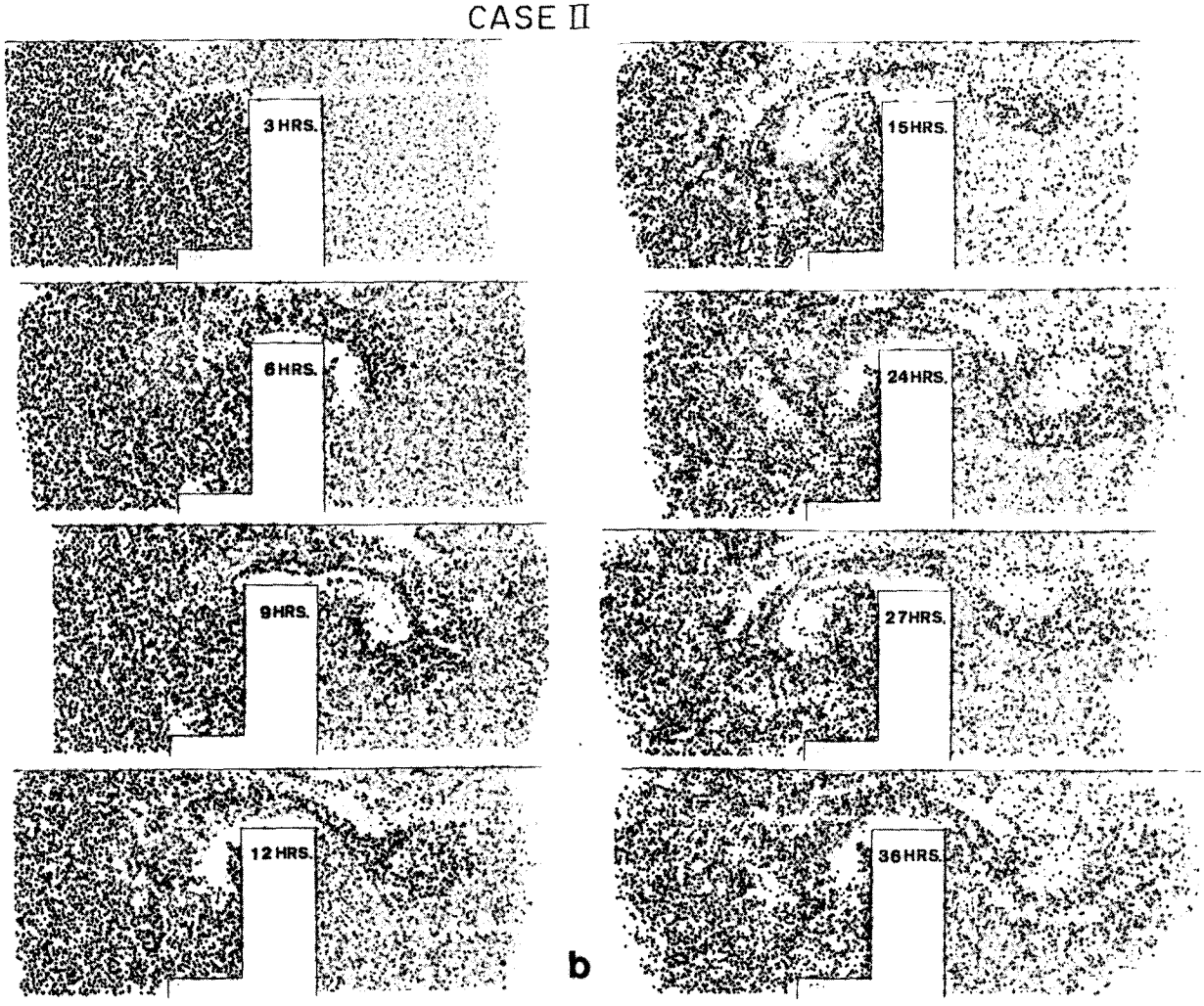

FIG. 2. (*Continued*)

squares having a side of 2 km are used in the present calculation of M_R.

Fig. 3 shows the distributions of the calculated M_R in cases I, II and III after a full cycle of the M_2 tide (all values of M_R are plotted in the initial positions of the specified particles). Since turbulent motions of particles are necessary for water mixing (Dyer, 1973), it is unreasonable to regard M_R in case I as a mixing ratio. Since non-zero values of M_R in case I are associated with deformation of water columns, which is one of the major factors in water mixing, it can be considered that M_R in case I indicates the degree of possible water mixing when turbulent motions are introduced into particle motions. It is easily seen in Fig. 3 that in all cases, values of M_R are largest in the vicinity of the strait, where some are over 0.9, and gradually decrease toward the inner parts of both basins. In cases II and III the areas of relatively large values of M_R, e.g., over 0.7 (shaded parts in Fig. 3), are more extensive than those in case I. The comparison of M_R between cases I and III is shown in Fig. 4, where the values of M_R in case III after a cycle are plotted against those in case I. Almost all of the plotted dots are distributed above the straight line at 45°. These figures clearly indicate that when turbulent motions are added to particles even if they are weak, local mixing is amplified to a great extent over a wide area around the strait.

Brief consideration concerning the cause of the above features of M_R is made, based on the Lagrangian movement of particles. Fig. 5 shows the initial and final positions of six groups of water particles during the first tidal cycle (each group consists of 16 particles). Initial positions of the groups are represented by the squares (1 km × 1 km) labeled by the letters U–Z, and final positions of 16 particles of each group are denoted by the corresponding small letters. Therefore, Fig. 5a (case I) represents the

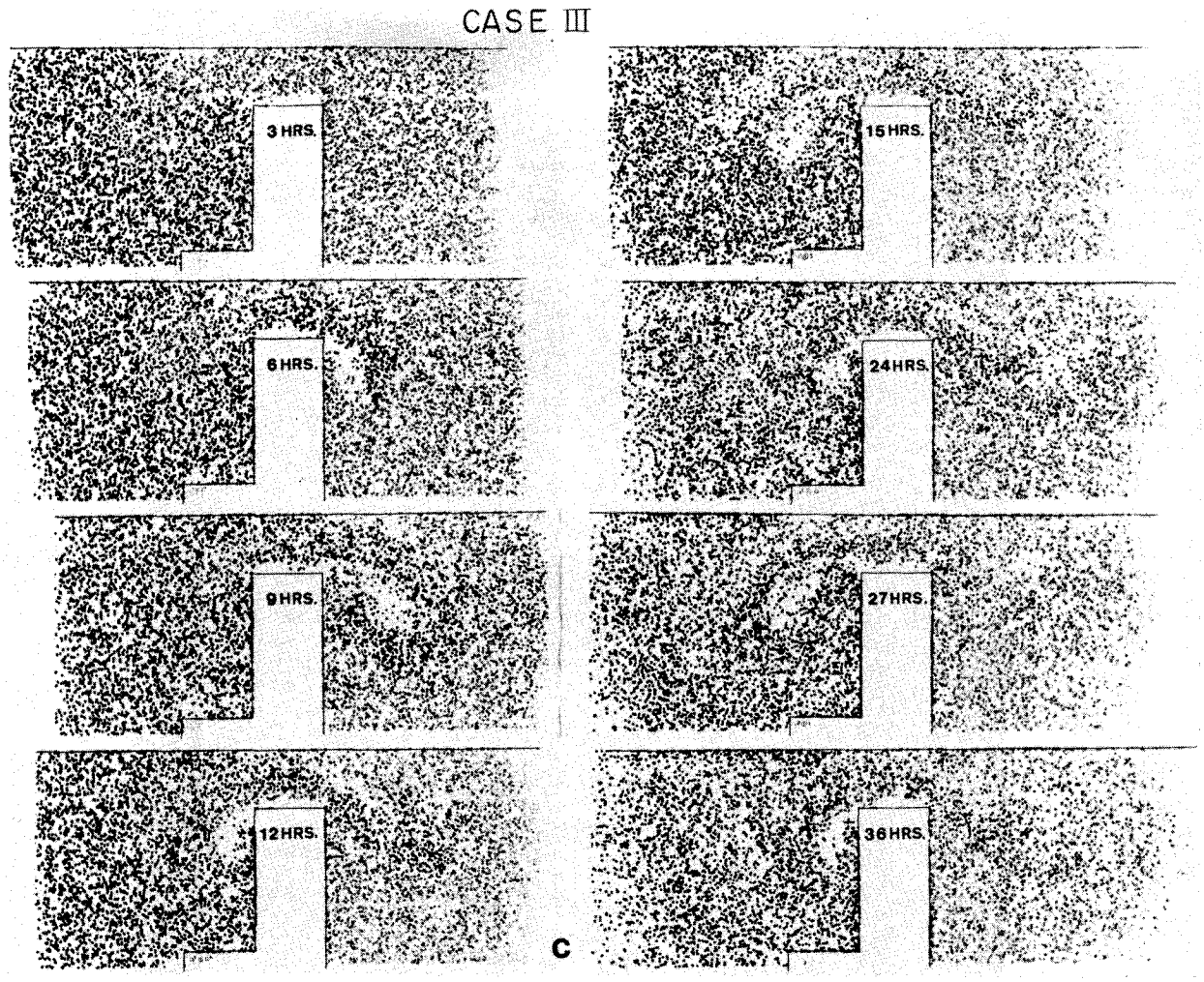

FIG. 2. (*Continued*)

deformation of a water column (the square) after a cycle due to the spatial variability of the velocity field. It is clearly seen in Fig. 5a that water columns in the vicinity of the strait are greatly deformed and some are stretched more than 5 km. The large deformation of water columns near the strait indicates the important fact that the Stokes drifts of two particles very close to each other in the vicinity of the strait are quite different. In other words, this fact causes the high values of M_R of case I in the vicinity of the strait and a large degree of the "apparent local mixing."

In Fig. 5b of the turbulent case (case III), it is also seen that particles released near the vicinity of the strait are scattered more widely than those in case I. The extensive scattering of the particles near the strait will be easily explained in comparison with trajectories of particles between the nonturbulent and turbulent cases. Fig. 6 demonstrates the trajectories of some representative particles in cases I (Fig. 6a; non-turbulent case) and III (Fig. 6b; turbulent case) during the first tidal cycle. In regions far from the strait, the trajectories in the turbulent case (Fig. 6b) only fluctuate around those in the non-turbulent case (Fig. 6a). However, the notable difference between these two cases is clearly observed in the trajectories of the particles that move near the strait during a cycle. Difference in the final positions of these particles between the two cases is well over 2 km, and, surprisingly, some particles (e.g., particle A in Fig. 6) in the turbulent case intrude into the opposite basin through the strait after a cycle, while in the non-turbulent case they remain in the home basin. From this large difference of final positions between the non-turbulent and turbulent cases, it is expected that in the vicinity of the strait, half of the particles released in a turbulent tidal current will have much larger drifts than Stokes particles (non-turbulent) and the other half much smaller drifts than Stokes particles over a cycle because of the ran-

domness of turbulence. Both the former and the latter particles will induce extensive scattering of water particles moving in a tidal current. In fact, these features can be seen in a comparison between Figs. 5a and 5b; the latter clearly shows that a group of particles initially included in a square (1 km × 1 km) in the vicinity of the strait is scattered more extensively after a cycle than the large deformation of water columns demonstrated in Fig. 5a, and that local mixing increases over a wide area around the strait, compared with that due only to turbulence. Since the scattering of the particles included in a square due only to turbulence of case III is ~1 km over a cycle, the extensive scattering near the strait cannot be explained only by turbulence.

Particles near the strait in the turbulent case do not fluctuate around their trajectories in the non-turbulent case but follow trajectories quite different from those in the non-turbulent case. In other words, we can consider the following process. Particles momentarily shift from the non-turbulent trajectory of one particle to that of another particle through the working of turbulence. Since the spatial difference between Stokes drifts is large in the vicinity of the strait, particles released near the strait in the turbulent case finally have "drifts" quite different from those in the non-turbulent case (Stokes drifts) and approach other particles initially at large distances. This phenomenon becomes especially remarkable for particles that pass through the strait. Hence, it is concluded that in the vicinity of the strait a large degree of local mixing is induced by the cooperation of the Stokes drifts in a tidal current (induced by the spatially rapid changes of the amplitude and the phase lag) and turbulence.

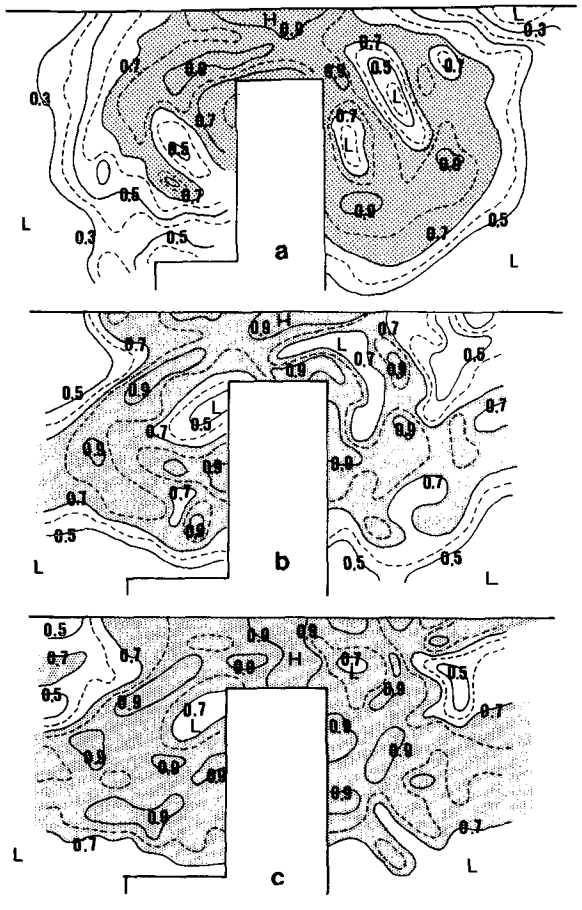

FIG. 3. The distributions of the calculated M_R after a cycle of the M_2 tide: (a) case I, (b) case II and (c) case III. The values of M_R are plotted at the initial positions of the specified particles. Shaded parts show the areas where the values of M_R exceed 0.7.

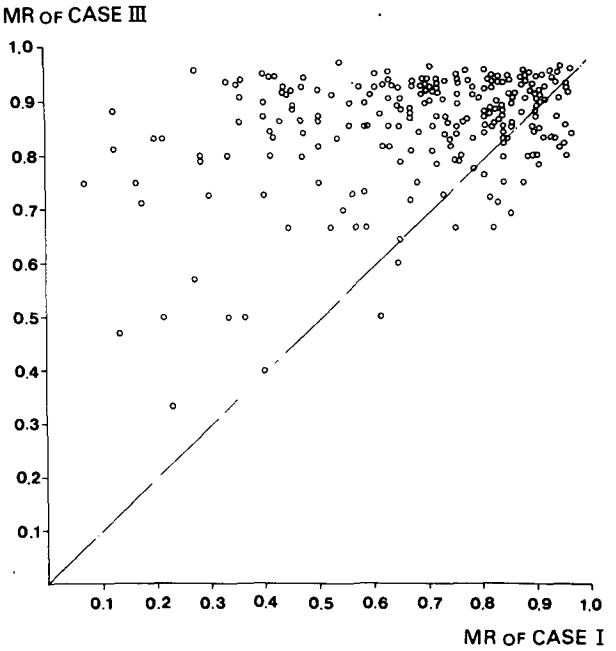

FIG. 4. Comparison of M_R in case III with that in case I after a cycle of the M_2 tide. The dot-dashed line is at 45°.

b. *Mixing of the inner and outer waters*

Based on the physical process of local mixing described in the preceding section, the mixing of the inner and outer waters initially separated from each other by the strait will now be discussed.

First, the degree of mixing of the inner and outer waters is estimated. Fig. 7 shows the horizontal distributions of the ratio N_R of the number of the outer water particles to the total number of particles in each grid box after three tidal cycles in cases I and III. Since the value (0.5) of N_R in case I (Fig. 7a; non-turbulent case) indicates that the inner and outer waters stay close together in a grid box, the increase of areas of the values close to 0.5 indicates that the contact surface of these two waters is increased only by tidal exchange through the strait or the defor-

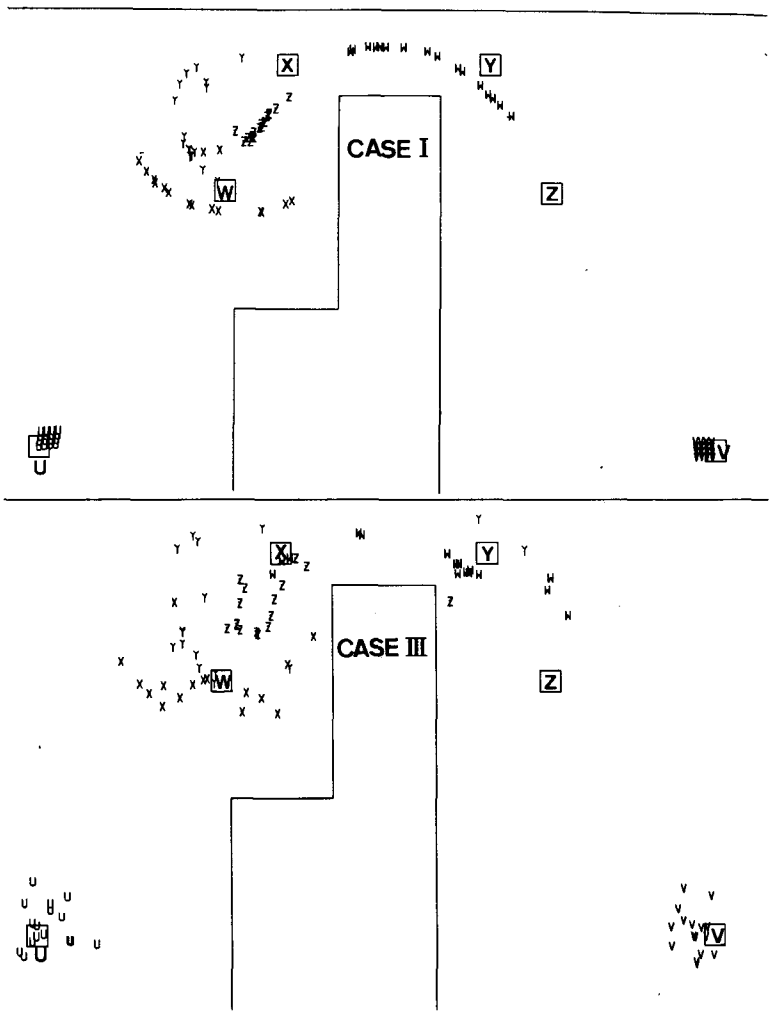

FIG. 5. The final positions (small letters) of 16 particles released initially in a square of 1 km × 1 km (corresponding capital letter in the square) in cases I and III over a cycle. In case I small letters represent the deformation of a water column, and in case III they represent the scattering of water particles included initially in the square.

mation of water columns because of a lack of turbulence. On the other hand, the values close to 0.5 in case III (Fig. 7b; turbulent case) may be considered as indicating that the inner and outer waters are well mixed in grid boxes. In Fig. 7, the values of 0.4 ~ 0.6 of N_R (shaded parts) are observed in a broad area near the strait in both cases. The differences between both cases are easily detected; i.e., the distribution of N_R in case III is very gentle in space, and in addition in case III the values of 0.4 ~ 0.6 are observed in wider areas than those in case I. These features clearly show that the inner and outer waters are well mixed with each other over an extensive area around the strait and that the physical process of water exchange through the strait is necessary for the mixing of these two waters.

The physical process of the mixing of the inner and outer waters can be understood as follows. During the first tidal cycle, as is demonstrated in Fig. 2, the greater part of the particles move together with fellow water particles (e.g., water particles released initially in the inner basin); therefore, the mixing of the inner and outer waters occurs only in narrow regions near their boundaries in the vicinity of the strait (the figure at $t = T$ in Fig. 2c, where T is a cycle of M_2). Fig. 8 shows the final positions ($t = T$) of the inner water particles extruding to the outer basin at the end of the first cycle (Fig. 8a), and the initial positions ($t = 0$) of the outer water particles intruding into the inner basin at the end of the first cycle (Fig. 8b). The region of the former positions is called R_1 and that of the latter ones R_2. During the second cycle, particles staying in R_2 are driven to the inner basin through the strait. In the

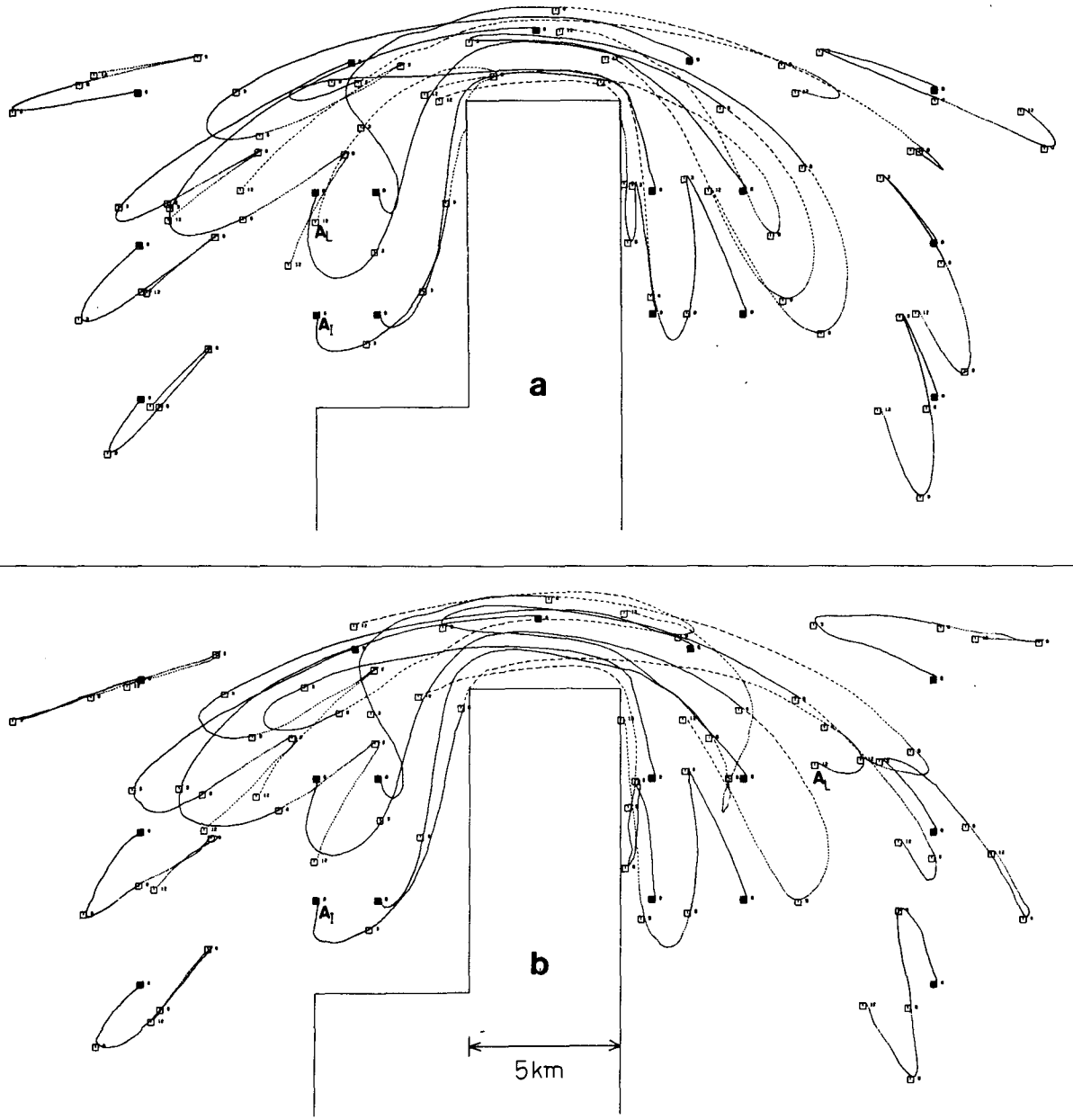

FIG. 6. The trajectories of some representative particles during the first tidal cycle: (a) case I and (b) case III. The small black squares represent the initial positions of the particles.

region R_2 at time $t = T$, the inner and outer water particles stay, since there is an overlapping part (R_3) of R_1 and R_2 as can be easily seen in Fig. 8; the inner water particles stay in the overlapping part R_3 and the outer water particles stay in the region R_2 except for the overlapping part R_3. Therefore these inner and outer water particles in the region R_2 are driven together to the inner basin through the strait, and they are well mixed with each other at the end of the second cycle, because of the strong local mixing in the vicinity of the strait. It is important in strong tidal mixing of the inner and outer waters that the region R_2 overlaps with the region R_1; this should be noted. The other inner water particles moving to the outer basin at time $t = T$ stay in the region R_1 except for the overlapping part R_3. Since these inner water particles move through regions near the strait during the second cycle, they are also considerably well mixed with the outer water around them. These are the same in the mixing process of the outer water

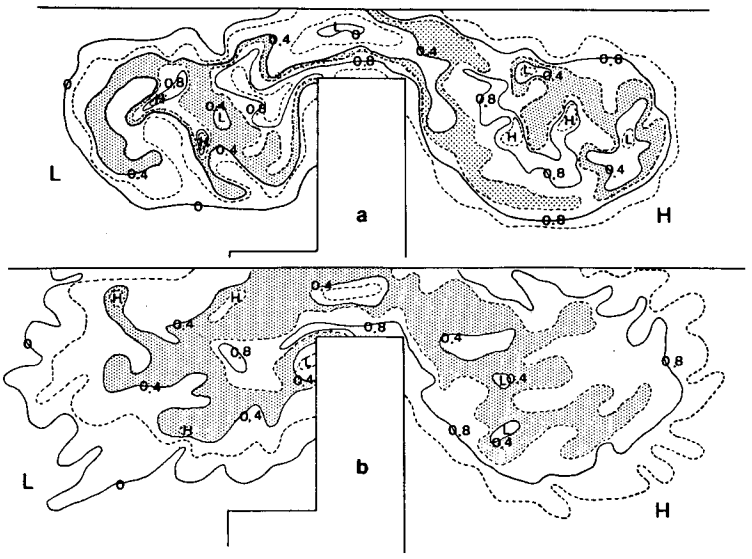

FIG. 7. The distributions of the calculated N_R after three tidal cycles: (a) case I and (b) case III. Shading denotes the areas where the values of N_R are from 0.4 to 0.6.

intruding into the inner basin at $t = T$ with the inner water. The above process is continued in subsequent cycles, and the mixing of the inner and outer waters is further developed.

Thus, strong mixing of the inner and outer waters is caused over an extensive area around the strait by the combined actions of a large degree of local mixing induced by the Stokes drift and turbulence, and the dynamic process of tidal exchange through the strait.

4. The effect of turbulence on tidal exchange through the strait

First the exchange ratios in the turbulent and non-turbulent cases are considered. According to Awaji *et al.* (1980), the exchange ratio R_n in the nth tidal cycle of the M_2 tide is defined as

$$R_n = V_{n,\mathrm{res}}/V_{n,\max}\,, \qquad (6)$$

where $V_{n,\max}$ denotes the maximum volume of the outer water existing in the inner basin in the nth tidal cycle and $V_{n,\mathrm{res}}$ the volume of the outer water remaining in the inner basin at the end of the nth cycle. Values of $V_{n,\max}$ and $V_{n,\mathrm{res}}$ are obtained from the proportion of the number of the outer water particles to the total number of water particles in every grid box in the inner basin.

The calculated values of $V_{n,\max}$, $V_{n,\mathrm{res}}$ and R_n are given in Table 1. By comparing the above values for cases I, II and III, we find only minor differences between the exchange ratios R_n in the turbulent cases (cases II and III) and in the non-turbulent case (case I) during three tidal cycles; and the values of $V_{n,\max}$ and $V_{n,\mathrm{res}}$ are also nearly equal in all cases. These facts seem curious, but they arise from the nature of turbulence, i.e., the probability of an outer water particle intruding into the inner basin in the turbulent case but returning to the outer basin in the non-turbulent case after a cycle is nearly equal to that of the opposite phenomenon, because of the turbulent motion of the particle. The above facts are correct during three tidal cycles. The data are insufficient, however, to extend the conclusion over many tidal cycles.

The dependence of sea areas affected by tidal exchange on turbulence is now considered. Fig. 9 shows the distributions of the initial positions ($t = 0$) of the inner and the outer water particles flowing into the outer and inner basins after three tidal cycles, respectively, and the distributions of their final positions ($t = 3T$) in cases I and III. It is clearly seen in Fig. 9 that the areas of the former and the latter distributions in case III are more extensive than those in case I, where the boundaries of the areas in case III extend ~3 km beyond those in case I. The above phenomenon is due to the drifts of water particles larger than the Stokes drifts in the turbulent case as mentioned in Section 3a (the extension of boundaries of the areas due only to turbulence in case III is expected to be at most 1.5 km beyond those in case I over three cycles). More extensive areas concerned with tidal exchange through the strait in case III indicate that in turbulent cases the particles released far from the strait are able to intrude into the opposite basin through the strait, and the intruding particles are distributed to the more inner parts of the basin, compared with those in non-turbulent cases. Then, material circulation between two basins

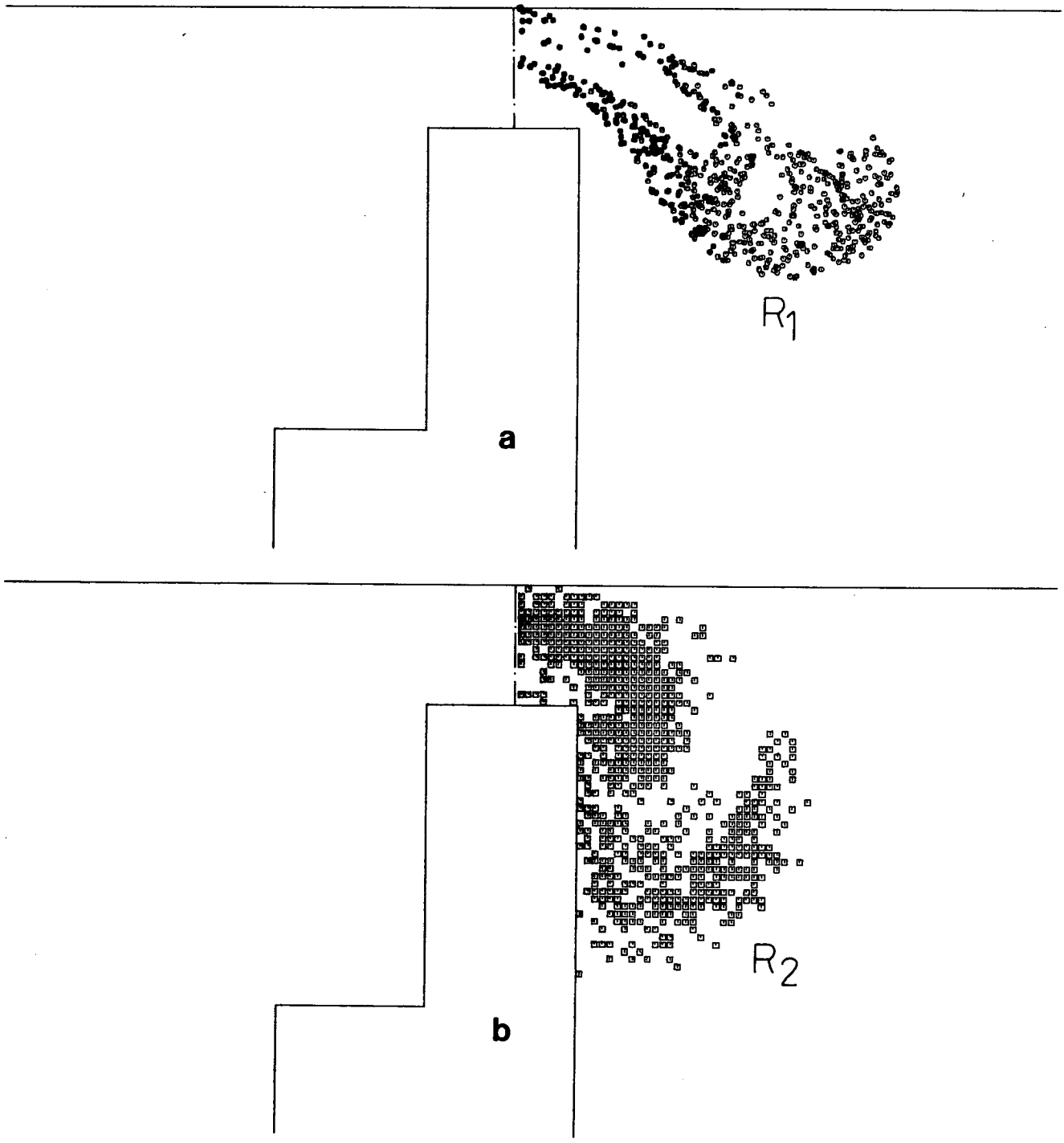

FIG. 8. (a) The final positions ($t = T$) of the inner water particles drawn out to the outer basin at the end of the first tidal cycle, and (b) the initial positions ($t = 0$) of the outer water particles intruding into the inner basin at the end of the first tidal cycle.

connected by a strait is accelerated in turbulent cases, in spite of the small difference between amounts of tidally induced net exchanges of water through the strait in the turbulent and non-turbulent cases.

To sum up, turbulence has a minor influence on water volumes exchanged between basins connected by a strait, but, working with a tidal current, it has a major influence on the enlargement of sea areas affected by tidal exchange through a strait.

TABLE 1. The calculated values of V_{max}, V_{res} and R.

		Case I	Case II	Case III
1st tidal cycle	V_{max} ($\times 10^7 m^3$)	214	210	211
	V_{res} ($\times 10^7 m^3$)	186	185	180
	R (%)	86.9	88.1	85.3
2nd tidal cycle	V_{max} ($\times 10^7 m^3$)	288	292	295
	V_{res} ($\times 10^7 m^3$)	198	200	201
	R (%)	68.8	68.4	68.1
3rd tidal cycle	V_{max} ($\times 10^7 m^3$)	316	328	325
	V_{res} ($\times 10^7 m^3$)	235	248	247
	R (%)	74.4	75.6	76.0

5. Dispersion coefficient

Almost all of the studies on water dispersion have been concerned with shear dispersion generated by the combined effects of turbulence and velocity shear (Bowden, 1965; Okubo, 1967). As was clearly shown by Awaji *et al.* (1980) and in the present study, a large amount of water is exchanged through the strait by the tidal current alone. This means that extensive water dispersion can be induced just by the large Stokes drifts near the strait even if there is no turbulence (it must be noticed that the velocity of the tidally induced residual current is small in the interior of the strait). Such a remarkable effect of the Stokes drift on water dispersion has not been clearly considered in shear dispersion theory. There are a few studies on water dispersion caused by the Stokes drift (Zimmerman, 1979), in which the Stokes drift in a tidal current having spatially small gradients in the velocity field was treated. The assumptions made in such studies concerning the Euler-Lagrange approximation, however, are inappropriate in the present case because of the spatially rapid changes in the velocity field of the tidal current. The combined actions of the Stokes drift and turbulence induce the more extensive dispersion of water particles in a tidal current.

The dispersion coefficient is evaluated by calculating the variance of the spread of particles (16 particles) released in each grid box near the strait. Fig. 10 shows the distributions of the calculated dispersion coefficients in cases I and III, where they are plotted at the initial centers of the 16 particles. In both cases, dispersion coefficients are over 10^6 cm^2 s^{-1} (shaded parts in Fig. 10) in the vicinity of the strait. In case III, especially, dispersion coefficients over 10^6 cm^2 s^{-1} are observed in wider areas than those in case I and some of them almost reach 8

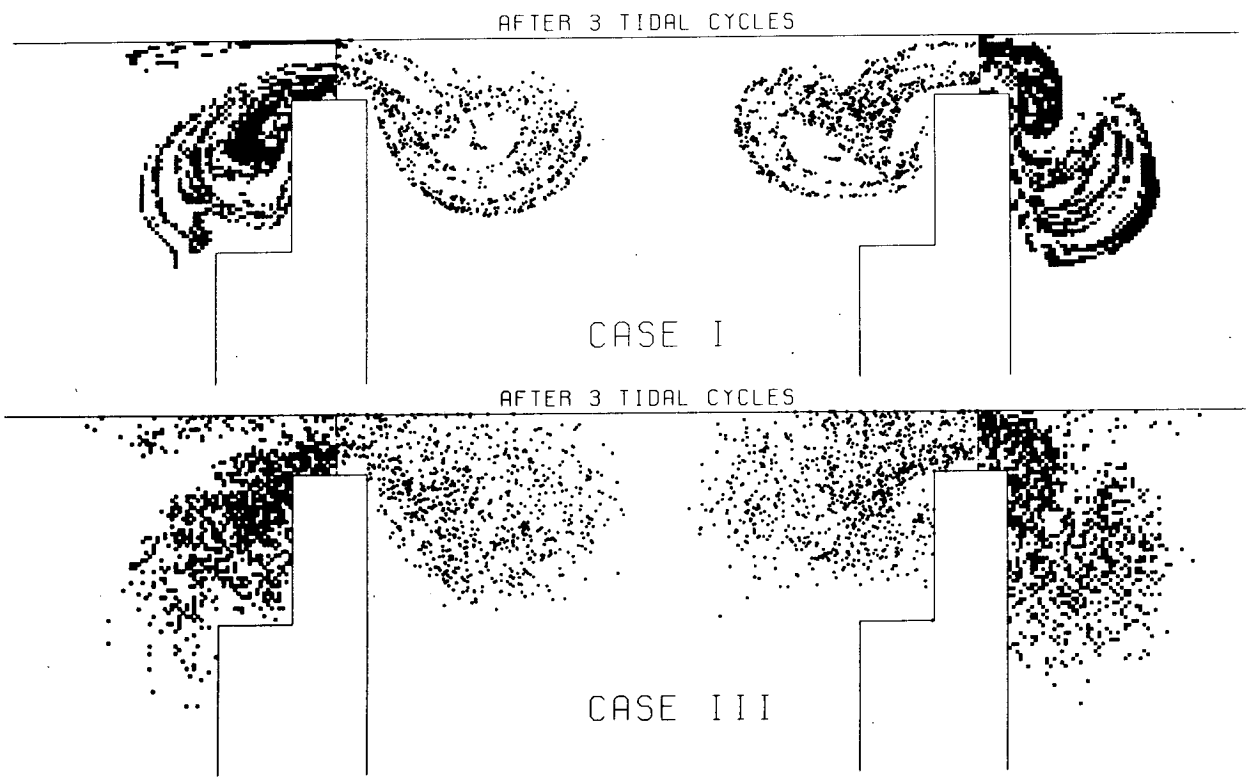

FIG. 9. The initial positions (t = 0, denoted by squares) and the final positions (t = 3T, denoted by circles) of the inner water particles drawn out to the outer basin after three tidal cycles (the left side), and those of the outer water particles intruding into the inner basin after three tidal cycles (the right side): (a) case I and (b) case III.

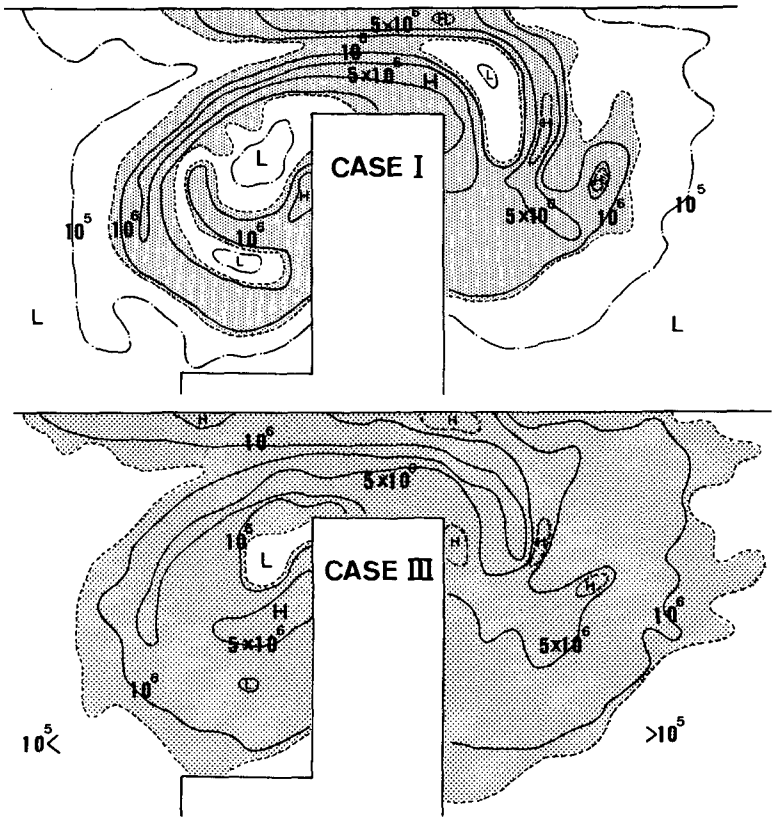

FIG. 10. The distributions of the calculated dispersion coefficients in cases I and III after one tidal cycle. Shading denotes the areas where the dispersion coefficients are over 10^6 cm^2 s^{-1}. Dotted lines represent isopleths of 8×10^6 cm^2 s^{-1}.

$\times 10^6$ cm^2 s^{-1}. These values are much higher than the value of the genuine dispersion coefficient (10^5 cm^2 s^{-1}) given in case III. Fig. 10 clearly shows that values of dispersion coefficients over 10^6 cm^2 s^{-1} are produced by the Stokes drift and that turbulence increases them by one order of magnitude in combination with the Stokes drift.

In the present study the mechanism of tidal mixing and the effect of turbulence on tidal exchange are investigated by using the Euler-Lagrange method. On performing the calculation of the Lagrangian movement of water particles by means of the Euler-Lagrange method, there are some problems which should be improved, especially in regard to interpolation of Eulerian velocities calculated at grid points. Small areas containing no particles are observed in Fig. 2. Such small blanks appear in another calculation using a finer grid size, but the area of the blanks is relatively small although this calculation is not demonstrated in the present paper. A major cause of occurrence of the blanks consists in the present interpolation method (a weighted linear interpolation) in calculating Lagrangian velocities of particles from Eulerian velocities at grid points surrounding the particles (see Awaji *et al.*, 1980). In the vicinity of the strait the Eulerian velocity field of the tidal current is strongly nonlinear. In this case the present linear interpolation will produce errors in the calculation of the Lagrangian movement of particles. It may be thought, however, that the errors are not so large as to invalidate the results in the present study. Recently, methods suitable for interpolation of Eulerian velocities in nonlinear velocity fields, such as the spline technique (Cox, 1978; and others), have been developed. Further studies on the Lagrangian movement using better interpolation methods will be needed.

Acknowledgments. I wish to express my hearty thanks to Prof. N. Imasato of the Geophysical Institute of Kyoto University for his discussions and critical reading of this paper. I am also grateful to Prof. H. Kunishi for his encouragement, and also to Dr. A. Wada for his suggestions on the generation of turbulence. The numerical calculations in the present study were carried out on the FACOM M-190 and M-200 in the Data Processing Center of Kyoto University. A part of the present study was supported by the scientific fund 446039 of the Japanese Ministry of Education.

APPENDIX

Generation of Turbulence by a Markov-Chain Model

According to a Markov-chain model (Hall, 1975), one component $u'(t_i)$ of the turbulent vector experienced by a labeled particle during the time step from t_i to t_{i+1} is given by

$$u'(t_i) = \rho u'(t_{i-1}) + \gamma(t_{i-1}), \tag{A1}$$

where ρ is a constant given by Eq. (A2), and γ is a random variable chosen from a Gausian distribution with a mean value of zero and a standard deviation of σ and is numerically generated; γ is independent of all $u'(t_i)$. The correlation $R(m\Delta t)$ between turbulent velocities separated by m time steps is ρ^m. Therefore, when the time interval $\Delta t \ll T_L$ (where $T_L = \int_0^\infty R(\xi)d\xi$ is the integral time scale), the constant ρ is approximated as

$$\rho = \exp(-\Delta t/T_L). \tag{A2}$$

Taking the variance of both sides of Eq. (A1), the standard deviation σ is given by

$$\sigma = \sigma_v(1 - \rho^2)^{1/2}, \tag{A3}$$

where σ_v is the standard deviation of the turbulent velocities. Therefore, if σ_v is known, a sequence of turbulent velocities experienced by a labeled particle is obtained from Eq. (A1). The standard deviation σ_v is determined according to the relation between σ_v and the diffusion coefficient K as follows. When time t is large compared with T_L, the variance of particle spread Φ is approximated as

$$\Phi \approx 2\sigma_v^2 T_L t. \tag{A4}$$

Then the diffusion coefficient K is given by

$$K = 0.5d\Phi/dt \approx \sigma_v^2 T_L . \tag{A5}$$

Thus when T_L and K are known, σ_v is obtained from Eq. (A5).

The variance Φ is rewritten from Eq. (A5) as

$$\Phi = 2Kt. \tag{A6}$$

In Section 5, the variance Φ is calculated from the distributions of particles, and using this variance Φ, the dispersion coefficient is evaluated from Eq. (A6).

REFERENCES

Awaji, T., N. Imasato and H. Kunishi, 1980: Tidal exchange through a strait: A numerical experiment using a simple model basin. *J. Phys. Oceanogr.*, **10,** 1499–1508.

Bowden, K. F., 1965: Horizontal mixing in the sea due to a shearing current. *J. Fluid Mech.*, **21,** 83–95.

Cox, M. G., 1978: The numerical evaluation of a spline from its *B*-spline representation. *J. Inst. Math. Appl.*, **21,** 135–143.

Dyer, K. R., 1973: *Estuaries: A Physical Introduction.* Wiley, London, 140 pp.

Hall, C. D., 1975: The simulation of particle motion in the atmosphere by a numerical random-walk model. *Quart. J. Roy. Meteor. Soc.*, **101,** 235–244.

Imasato, N., T. Awaji and H. Kunishi, 1980: Tidal exchange through Naruto, Akashi and Kitan Straits. *J. Oceanogr. Soc. Japan*, **36,** 151–162.

Kawamura, M., K. Shimizu, H. Koyama, H. Nakajima and T. Maekawa, 1975: Hydrographic conditions and diffusion coefficient in the Bungo Channel. *Umi To Sora*, **50,** 43–58.

Longuet-Higgins, M. S., 1969: On the transport of mass by time-varying ocean currents. *Deep-Sea Res.*, **16,** 431–447.

Okubo, A., 1967: The effect of shear in an oscillatory current on horizontal diffusion from an instantaneous source. *Int. J. Oceanol. Limnol.*, **1,** 194–204.

Parker, D. S., D. P. Norris and A. W. Nelson, 1972: Tidal exchange at Golden Gate. *ASCE J. Sanitary Div.*, **98,** 305–323.

Sullivan, P. J., 1971: Longitudinal dispersion within a two-dimensional turbulent shear flow. *J. Fluid Mech.*, **49,** 551–576.

Wada, A., and M. Kadoyu, 1975: The flow condition and the diffusion characteristics in the Seto Inland Sea. *Coastal Eng. Japan*, **18,** 143–154.

——, and ——, 1976: Numerical simulation on the motion of water particles in the Seto Island Sea. *Proc. 20th Japanese Conf. Hydraulics*, 191–196.

Zimmerman, J. T. F., 1976: Mixing and flushing of tidal embayments in the western Dutch Wadden Sea, II: Analysis of mixing process. *Netherlands J. Sea Res.*, **10,** 397–439.

——, 1979: On the Euler-Lagrange transformation and the Stokes' drift in the presence of oscillatory and residual currents. *Deep-Sea Res.*, **26,** 505–520.